Shao, L.H.; Ruther, M.; Linden, S.; Wegener, M.; Weissmueller, J.:

On the mechanism of electrochemical modulation of plasmonic resonances

In: Applied Physics Letters (2012) AIP

DOI: 10.1063/1.4753805

On the mechanism of electrochemical modulation of plasmonic resonances

L.-H. Shao,[1,2,3] M. Ruther,[2,3,4] S. Linden,[2,3,4,5] M. Wegener,[2,3,4] J. Weissmüller[1,6]

[1] *Institut für Werkstoffphysik und Werkstofftechnologie, Technische Universität Hamburg-Harburg, Hamburg, Germany*
[2] *Institut für Nanotechnologie, Karlsruhe Institute of Technology, Karlsruhe, Germany*
[3] *DFG-Center for Functional Nanostructures, Karlsruhe Institute of Technology, Karlsruhe, Germany*
[4] *Institut für Angewandte Physik, Karlsruhe Institute of Technology, Karlsruhe, Germany*
[5] *Physikalisches Institut, Universität Bonn, Bonn, Germany*
[6] *Institut für Werkstoffforschung, Werkstoffmechanik, Helmholtz-Zentrum Geesthacht, Geesthacht, Germany*

Recent electrochemical experiments on gold-based photonic metamaterials have shown a sizable reversible tuning and modulation of plasmonic resonances. Here, we study the mechanism of the electrochemical modulation by measuring the change of the resonance transmittance and resonance frequency during underpotential deposition of Pb, Cu and electrosorption of OH. The electric resistance change of the resonators is identified as decisive for the resonance transmittance change, while the space-charge layer at the metal surface shifts the resonance frequency.

Photonic metamaterials, for instance nanoscale metallic split-ring resonator (SRR) arrays [1,2,3], can provide the basis for unconventional optical response such as negative refraction [4], perfect lensing [5] and electromagnetic cloaking [6]. As these phenomena are often limited to a narrow and fixed spectral bandwidth, strategies for tuning the frequency, ideally by an electric signal, are desirable. For metallic metamaterials, the optical properties may be affected via space-charge layers, controlled by an applied electric potential. Along these lines, field-effect-transistor like structures have recently been discussed at far-infrared [7,8] as well as at optical frequencies [9]. A sizable reversible tuning and modulation of plasmonic resonances in optical metamaterials was achieved in our previous work, which used gold SRRs as the working electrode in an electrochemical cell [10]. The resonance position and damping was modulated, with the extinction peak shifting by as much as 18% of the center frequency or more than twice the damping for zero electrode potential. Here, we explore the mechanism behind the coupling of optical response and applied potential in metallic metamaterials. As the key approach, we use the underpotential deposition of monolayers of Cu, Pb, and OH on the gold SRR structures.

Broadly speaking, resonances in metamaterials are governed by geometry through inductivity and capacity, and by materials parameters through resistance and plasmon resonances. As discussed in reference [10], changes in geometry alone – as embodied in the space-charge induced shift of the image plane [11] – are not able to fully explain the observations. Furthermore, changes in the refractive index of the electrolyte have been ruled out as the prevailing mechanism behind electrochemical tuning of the optical response [10]. It is also known that space-charge regions at metal surfaces are screened within the outermost atomic layer. These findings direct our attention towards phenomena immediately at the metal surface, and it is natural to suspect a coupling between the optical response and the electrical resistance.

In fact, the experiments showed a pronounced effect of the electrochemical postprocessing. Along with a reduction in the roughness of the resonator surfaces, the resonance shifts to blue and the damping is diminished for the gold-film thicknesses from near the percolation threshold to 30 nm [10,12]. It is well known that the electron scattering – and, hence, the resistance – at the solid-electrolyte interface depend on the surface roughness, with lower resistance at smoother surfaces [13]. In other words, experiment correlates the reduction of the resonator resistance during electrochemical cycling with a modulation of the optical response. In support of our speculation, large potential-induced resistance changes have been observed in thin metal films, nanoporous metals and oxides [14,15,16,17,18].

Arrays of Au SRR were made by electron-beam lithography on indium tin oxide (ITO)-coated glass slides using 2 nm Cr adhesion layer, see Ref. [10] for details. An example of a 10 nm thin gold structure is shown in the inset in Fig. 1 All samples in this study had similar SRR edge lengths ~90 nm, while the SRR thickness–which could be measured by atomic-force microscopy–was varied. The electrochemical experiments were performed in a quartz glass cuvette. The glass slides sample were immersed in electrolyte, with the ITO film and SRR arrays serving as the working electrode and Au wire forming the counter electrode. Electrode potentials were measured relative to Ag/AgCl in saturated KCl solution. Normal incidence transmittance spectra were measured in situ. Before any measurement, all of the SRR samples are "trained" by electrochemical cycling. This procedure (see Refs. [10,12] for details) drastically enhances the resonances by improving the contiguity of the film and reducing its roughness.

Underpotential deposition (UPD) refers to the electrodeposition of a metal monolayer on a foreign metal substrate at potentials positive with respect to that for bulk deposition on the same metal surface [19-22]. The process depends on the surface orientation and defect structure, for instance, Pb initially decorates step edges [23,24]. We studied Pb and Cu UPD as well as the adsorption of a monolayer of OH on 10 nm thick SRR samples. Electrolytes were aqueous (ultrapure 18.2 MΩ cm grade water) solutions of 5 mM $CuSO_4$ + 0.1 M H_2SO_4 (Cu UPD), 1 mM $Pb(NO_3)_2$ + 0.1 M NaOH (Pb UPD), and in 0.7 M NaF solution (OH electrosorption). The UPD signatures are weak in the in-situ experiments with the metamaterial, since the resonators cover only a small area fraction of the electrode. Therefore, the potential intervals of the in-situ experiments were determined from electrochemical experiments on glass slides covered entirely with Au, using otherwise identical conditions as with the

metamaterial electrodes. In this way, the electrosorption signatures of the UPD processes could be mapped. Precise control of the negative vertex potential was particularly important, so that bulk deposition of Cu or Pb could be avoided. Cyclic voltammograms (CVs) of bare ITO substrates are featureless, consistent with capacitive double charging/discharging. Transmittance spectra recorded during those experiments show no change, confirming the absence of UPD on ITO. The electrosoprtion of OH was studied on the samples with different thicknesses are measured in 0.7 M NaF solution in the potential range from –0.9 V and 0.9 V.

As a first test of the link between resistance and frequency, we plot in Fig. 1 the variation of the resonance frequency, ω_R, of the metamaterial with the SRR thickness, d. The lateral dimensions of the SRRs are identical for all samples. A linear variation of ω_R with inverse film thickness is apparent. This agrees with the variation of the resistance, which scales with $1/d$. Note, however, that the variation of ω_R with d is weak, with a relative change in ω_R by ~25% while $1/d$ varies by the factor 2.5.

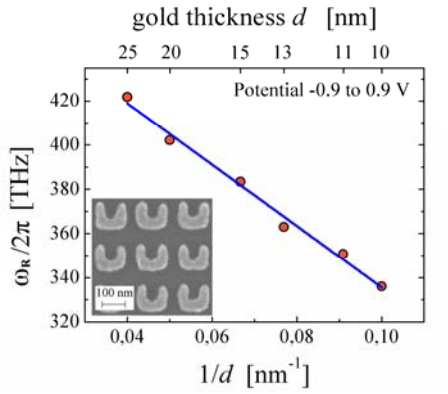

FIG.1. The resonance frequency ω_R of the SRR arrays (scanning electron micrograph shown as inset) versus the inverse $1/d$ of the resonator thickness. The line is a linear fit of the data points.

Figure 2 displays results of the experiments with Pb UPD on a Au foil. Fig. 2(a), shows the familiar signatures with the Pb sub-monolayer deposition starting at –0.2 V, followed by deposition peaks at –0.4 V, –0.55 V and –0.75 V. The last-mentioned peak corresponds to the completion of a full Pb monolayer [22]. At this point, the potential scan direction was inverted, and three corresponding desorption peaks can be identified in the positive-going scan, with the clean surface recovered after the last desorption peak at –0.4 V. The potential range for the in-situ experiments was then chosen as 0 V to –0.76 V.

Transmittance spectra of the 12 nm thick metamaterial (10 nm Au + 2 nm Cr) are shown in Fig. 2(b), while the variation of resonance transmittance T_R and resonance frequency ω_R with the electrode potential E are plotted in Fig. 2 (c) and (d), respectively. The measured spectra can be smoothed using the adjacent averaging method, then from potential of the minimum in the smoothed data set we can get T_R and ω_R. A large resonance peak shift can be observed, and both T_R and ω_R scale with the potential. In Fig. 2 (c) and (d), there is a turning point at $E = –0.4$ V, where the first deposition and last desorption peaks are. The resonance frequency ω_R stays at constant value at the most negative potentials, i.e. $E \leq –0.72$ V, which means one monolayer Pb has been deposited on the Au surface. A hysteresis in the potential-dependence of the optical properties maps the adsorption/desorption hysteresis of the CVs.

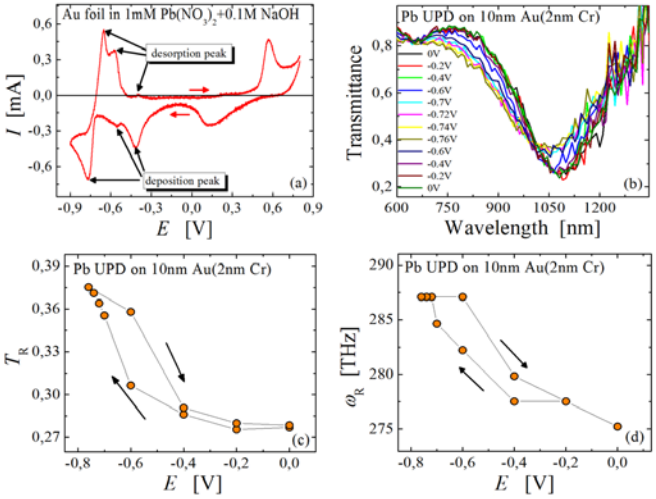

FIG.2 Pb underpotential deposition on gold in 1 mM $Pb(NO_3)_2$ + 0.1 M NaOH aqueous electrolyte. (a) Cyclic voltammogram measured on a gold foil. (b) to (d) In-situ optical measurement results of arrays of 10-nm thin gold split-ring resonators during UPD process. (b) Normal-incidence transmittance spectra. (c), (d) The corresponding resonance transmittance T_R and frequency ω_R *vs*. potential E.

The data shown in Fig. 3 are similar to those in Fig. 2, but for Cu UPD. The CV on a Au film in Fig. 3(a) shows adsorption / desorption peaks at $E = \sim 0.3$ V, and a broad shoulder at smaller potentials. The optical data of the metamaterial are shown in Fig. 3 (b) to (d). Overall, the effect of Cu UPD on the optical response is significantly weaker than that of Pb UPD. Yet, the impact of electrochemical cycles is measurable even for Cu UPD. Specifically, the resonance transmittance curve as shown in Fig. 3 (c) changes its slope at $E = \sim 0.3$ V, where the adsorption/desorption peaks are observed.

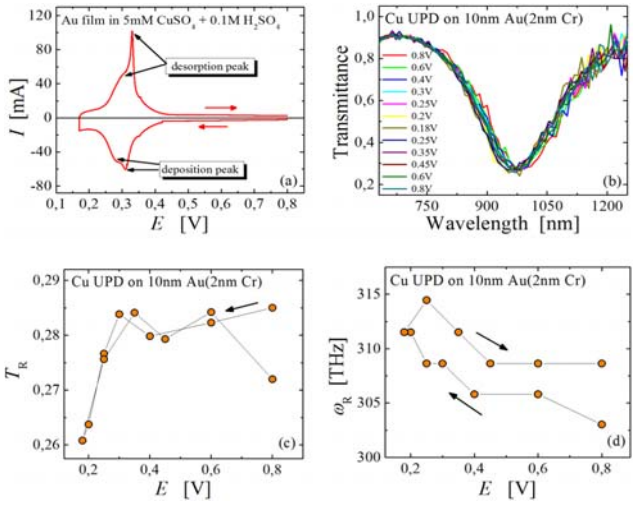

FIG.3. Cu underpotential deposition on gold in 5 mM $CuSO_4$ + 0.1 M H_2SO_4 aqueous electrolyte. (a) Cyclic volt-

ammogram measured on 30 nm thin Au film on glass substrate. (b) to (d) In-situ optical measurement results of arrays of 10-nm thin gold split-ring resonators during UPD process. (b) Normal-incidence transmittance spectra. (c), (d) The corresponding resonance transmittance T_R and frequency ω_R versus potential E.

As introduced in Ref. [10], the most important features of the CVs with Au SRRs in NaF electrolyte (Fig. 4(a)) are the OH-adsorption peaks during positive-going scans and the corresponding desorption peaks during negative-going scans in the potential range $E > 0$, which can also be treated as an OH UPD process. The optical data of the metamaterial are shown in Fig. 4 (b) to (d). Overall, the effect of OH UPD on the optical response is significantly larger than that of Cu UPD.

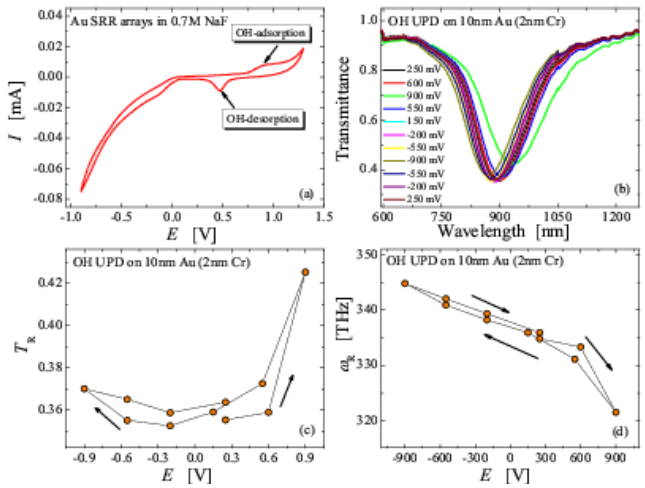

FIG.4. OH underpotential deposition on an array of 10 nm thin gold SRRs in 0.7 M NaF aqueous electrolyte (a) Cyclic voltammogram measured with potential range from –0.9 to +1.3 V. (b) to (d) In-situ optical measurement results during UPD process. (b) Normal-incidence transmittance spectra. (c), (d) The corresponding resonance transmittance T_R and frequency ω_R versus potential E.

The resistance change of the resonators of the present work in the photonic metamaterial is unknown. However, resistance changes have been reported for thin gold films subject to different electrochemical processes, including OH electrosorption as well as Pb and Cu UPD [14,15]. The variation are around 1 − 10%, depending on the nature process, for films around 30 nm thick. The SRR of the present study were significantly thinner, around 10 nm, so that we can assume that they suffer even larger resistance changes.

Table 1 Resistance, resonance transmittance and frequency change during underpotential deposition of different anions. R is the resistance of a thin gold film. The relative resonance transmittance and frequency changes of Au resonators are $\Delta\omega_R/\omega_{avg}$ and $\Delta T_R/T_{avg}$, respectively. The sign of the derivatives $\delta T_R/\delta\theta$, $\delta\omega_R/\delta\theta$ and $\delta(\Delta R/R)/\delta\theta$ are listed to show the trends of how T_R, ω_R and also the resistance $\Delta R/R$ change with the adsorbates coverage θ, and the sign of $\delta\omega_R/\delta E$ shows the trend of how ω_R changes with the applied potential E.

	$\frac{\Delta R}{R}$ %	$\frac{\Delta T_R}{T_{avg}}$ %	$\frac{\Delta\omega_R}{\omega_{avg}}$ %	$\frac{\delta\Delta R/R}{\delta\theta}$	$\frac{\delta T_R}{\delta\theta}$	$\frac{\delta\omega_R}{\delta\theta}$	$\frac{\delta\omega_R}{\delta E}$
OH/Au	12.5[14]	28	7	+	+	-	-
Pb/Au	6[15]	30	4	+	+	+	-
Cu/Au	1.2[15]	7	<2	-	-	+	-

Table 1 summarizes the most important observations from our UPD experiments with Pb, Cu, and OH-adsorption on metamaterials, along with the corresponding resistance changes in thin films, Refs. [14,15]. We find it instructive to also inspect the trends of how T_R, ω_R and R change with the adsorbate coverage, θ, and with the electrode potential, E. To this end, Table 1 also shows the sign of the derivatives $\delta T_R/\delta\theta$, $\delta\omega_R/\delta\theta$, $\delta(\Delta R/R)/\delta\theta$, and $\delta\omega_R/\delta E$. The table suggests the following observations:

1st: The trends in T_R *vs*. θ agree with those of $\delta(\Delta R/R)/\delta\theta$.

2nd: All graphs of ω_R *vs*. E display similar trend, independent of the electrode process.

3rd: The effect of Cu UPD on both, ω_R and T_R, is much smaller than the effect of Pb UPD and OH UPD.

The 1st observation can be understood qualitatively by describing the resonance behavior of the SRR as LC- (inductance-capacitance) circuit [3]. An additional resistive part can account for dissipation by Ohmic and radiation loss channels [25,26]. By defining an effective resistance R, we can combine the Ohmic and radiation losses and expand the LC- to an LCR model [25]. The quality factor, Q, which determines the width of the resonance peak of an LCR-circuit, scales inversely with the resistance [27],

$$Q = \omega_R L/R\,. \qquad (1)$$

In other words, increasing the SRR resistance will lead to a more shallow optical resonance. This agrees with the trends observed in our experiments.

A more detailed investigation is as follows: In the LCR model, the magnitude of the admittance, Y, (current amplitude over voltage amplitude for a sinusoidal excitation) is

$$|Y| = 1/\sqrt{R^2 + (\omega L - 1/\omega C)^2} \qquad (2)$$

The limiting behavior for $\omega\rightarrow\omega_R$ is $Y\rightarrow 1/R$, which means the peak height of the amplitude of the admittance spectra is inversely proportional to the resistance. The transmittance spectra of our experiments are analogous to the admittance spectra in the LCR model. Hence, the transmittance at the resonance frequency is inversely proportional to the resistance. This reasoning agrees with the 1st of the above observations.

From the T_R *vs*. E curves, it can be found that the resonance transmittance, T, exhibits nearly no change during the capacitive charging process (in the double layer potential range). This suggests that the charge density variation is not the key factor governing the transmittance. Instead, T is

more dependent on the adsorption/desorption process. This is consistent with a larger effect of electrosorption on the resistance as compared to the effect of capacitive charging. However, below we shall argue that the resonance frequency is sensitive to the charge density.

The 2nd and 3rd phenomena, and in particular the shift of the resonance frequency can be explained as follows: Whereas ω_R can increase or decrease during adsorption, depending on the adsorbate, ω_R consistently decreases with increasing electrode potential, independent of the electrode process. Furthermore, whereas the transmittance changes are most pronounced in the potential intervals of adsorption/desorption, the resonance frequency varies continuously with E throughout the entire potential intervals under study and independently of adsorption processes. These observations might tentatively be rationalized in a picture that links the resonance frequency to the electron density in the metal.

In support of the above view is a Drude-model based theory in studies of electron-induced surface plasmon resonance shift [28,29]. The aforementioned studies also report a blue-shifted resonance upon electron injection or Pb UPD on gold rods or metal particles. The central aspects of the theory can be exposed as follows:

Within a free electron gas approximation, the dielectric behavior of gold is described in the Drude function [28]

$$\varepsilon(\omega) = \varepsilon_\infty - \omega_{pl}^2 \Big/ \left(\omega^2 + i\gamma\omega\right) \quad (3)$$

where the bulk plasma frequency is given by

$$\omega_{pl} = \sqrt{n_e e^2 / m\varepsilon_0} \quad (4)$$

with e the electron charge, m the effective mass, ε_0 the permittivity of vacuum, ε_∞ the high-frequency contribution from interband transitions, γ damping and n_e the electron density. The surface plasmon peak central frequency ω is obtained as [28,30]

$$\omega^2 = \omega_0^2 \, (1 + \Delta n_e / n_e) \quad (5)$$

with

$$\omega_0^2 = \omega_{pl}^2 \left(\varepsilon_\infty + (S^{-1} - 1)\varepsilon_m\right)^{-1} . \quad (6)$$

Here, ω_0 is the plasmon frequency for the charge-neutral surface, S is a shape-dependent depolarization factor and ε_m is the dielectric constant of the medium outside the surface. Thus, the resonance frequency shift is

$$\Delta\omega = \omega - \omega_0 = \omega_0 (\sqrt{1 + \Delta n_e / n_e} - 1) . \quad (7)$$

Equation (7) links the resonance frequency shift to the electron density change, Δn_e. An increase of Δn_e will lead to the increase of ω and $\Delta\omega$. Qualitatively, the predictions of the free electron plasma frequency agree with the shift of resonance frequency observed in our work.

For capacitive processes at electrode surfaces, charge density, q, and electrode potential are linked by the capacitance, c, as $c = q/E$. This implies that the largest electron density change, Δn_e, in a scan scales with the negative vertex potential, E^-. The respective values used here obey $E^-_{Cu/Au} < E^-_{Pb/Au} < E^-_{OH/Au}$ (positive potential range is used for Cu UPD), which means that the electron density change has following relation that $\Delta n_{eCu/Au} < \Delta n_{ePb/Au} < \Delta n_{eOH/Au}$. Indeed, the effect of Cu UPD on ω_R is much smaller than the effect of Pb UPD and OH UPD. Even though the resonance frequency is inversely proportional to its resistance as shown in Fig. 1, the small relative change of the frequency might be covered by the electron-induced effect.

In conclusion, we have presented further experimental data, enabling a better qualitative understanding of the mechanism of electrochemical modulation of plasmonic resonances. The electrochemically induced electric resistance change of the resonators has a decisive impact onto the resonance damping, hence onto the resonance transmittance, while the change in electron density appears to mainly influence the resonance frequency.

References

[1] V. M. Shalaev. Nature Photon., **1** (**2007**) 41.

[2] C. M. Soukoulis, S. Linden, M. Wegener. Science, **315** (2007) 47.

[3] S. Linden, C. Enkrich, M. Wegener, J. Zhou, T. Koschny, and C.M. Soukoulis. Science. **306** (2004) 1351.

[4] V. G. Veselago. Sov. Phys. Usp., **10** (1968) 509.

[5] J. B. Pendry. Phys. Rev. Lett., **85** (2000) 3966.

[6] J. B. Pendry, D. Schurig, D. R. Smith. Science, **312** (2006) 1780.

[7] H. T. Chen , W. J. Padilla , J. M. O. Zide , A. C. Gossard , A. J. Taylor , R. D. Averitt , Nature 2006 , 444 , 597 .

[8] H. T. Chen , W. J. Padilla , M. J. Cich , A. K. Azad , R. D. Averitt , A. J. Taylor , Nature Photon. 2009 , 3 , 148 .

[9] E. Feigenbaum , K. Diest , H. A. Atwater , Nano Lett.,**10** (*2010*) 2111-2116.

[10] L.-H. Shao, M. Ruther, S. Linden, S. Essig, K. Busch, J. Weissmüller, M. Wegener. Adv. Mater., **22** (2010) 5173.

[11] Y. Umeno, C. Elsasser, B. Meyer, P. Gumbsch, M. Nothacker, J. Weissmuller, and F. Evers, Epl 78 (1) (2007).

[12] M. Ruther, L.-H. Shao, S. Linden, J. Weissmüller, M. Wegener. Appl. Phys. Lett., **98** (2011) 013112.

[13] R. Tucceri. Surf. Sci. Rep., **56** (2004) 85.

[14] J.-P. Ganon, C. Nguyen, J. Clavilier. Surf. Sci., **79** (1979) 245.

[15] W.N. Hansen. Surf. Sci., **101** (1980) 109.

[16] S. Dasgupta, R. Kruk, D. Ebke, A. Hütten, C. Bansal, and H. Hahn. J. Appl. Phys., **104** (2008) 103707.

[17] P. Wahl, T. Traußnig, S. Landgraf, H.-J. Jin, J. Weissmüller, R. Würschum. J. Appl. Phys., **108** (2010) 073706.

[18] S. Dasgupta, S. Dehm, R. Kruk, H. Hahn. Acta Phys. Pol. A, **115** (2009) 473.

[19] D. M. Kolb. *In Advances in Electrochemistry and Electrochemical Engineering*. H. Gerisher, C. W. Tobias, Eds.. Wiley, New York. 11 (1978).

[20] R. Adzic. *In Advances in Electrochemistry and Electrochemical Engineering*. H. Gerisher, C. W. Tobias, Eds.. Wiley, New York. 13 (1984).

[21] A. Aramata. *In Modern Aspects of Electrochemistry*. J. O'M. Bockris, R. E. White, B. E. Conway, Eds.. Plenum Press, New York. 31 (1997).

[22] E. Herrero, L. J. Buller, H. D. Abruña. Chem. Rev., **101** (2001**)** 1897.

[23] M. P. Green, K. J. Hanson, D. A. Scherson, X. Xing, M. Richter, P. N. Ross, R. Carr, I. Lindau. J. Phys. Chem., **93** (1989) 2181.

[24] M. P. Green, K. J. Hanson, R. Carr, I. Lindau. J. Electrochem. Soc., **137** (1990) 3493.

[25] T. P. Meyrath, T. Zentgraf, H. Giessen. Phys. Rev. B, **75**, (2007) 205102.

[26] M. Husnik, M. W. Klein, N. Feth, M. König, J. Niegemann, K. Busch, S. Linden, M.Wegener. Nature Photon, **2** (2008) 614.

[27] P. R. Clement, W. C. Johnson. Electrical Engineering Science. Chapter 7 & 15. Robert E. Krieger Publishing company, Malabar, Florida. (1982).

[28] P. Mulvaney, J. Perez-Juste, M. Giersig, L. M. Liz-Marzan, and C. Pecharroman. Plasmonics, **1** (2006) 61.

[29] P. Mulvaney. Langmuir, **12** (1996) 788.

[30] Matthias Ruther. PhD thesis, Karlsruher Institut für Technologie, 2011.

We acknowledge support by the DFG-Center for Functional Nanostructures (subprojects A1.5 and A1.6) and by the Bundesministerium für Bildung und Forschung (project METAMAT).